

Landscape of an exact energy functional

Aron J. Cohen

Department of Chemistry, Lensfield Rd, University of Cambridge, Cambridge, CB2 1EW, UK

Paula Mori-Sánchez

*Departamento de Química and Instituto de Física de la Materia Condensada (IFIMAC),
Universidad Autónoma de Madrid, 28049, Madrid, Spain*

One of the great challenges of electronic structure theory is the quest for the exact functional of density functional theory. Its existence is proven, but it is a complicated multivariable functional that is almost impossible to conceptualize. In this paper, the asymmetric two-site Hubbard model is studied, which has a two-dimensional universe of density matrices. The exact functional becomes a simple function of two variables whose three dimensional energy landscape can be visualized and explored. A walk on this unique landscape, tilted to an angle defined by the one-electron Hamiltonian, gives a valley whose minimum is the exact total energy. This is contrasted with the landscape of some approximate functionals, explaining their failure for electron transfer in the strongly correlated limit. We show concrete examples of pure-state density matrices that are not v -representable due to the underlying non-convex nature of the energy landscape. For the first time, the exact functional is calculated for all numbers of electrons, including fractional, allowing the derivative discontinuity to be visualized and understood. The fundamental gap for all possible systems is obtained solely from the derivatives of the exact functional.

In 1964 Hohenberg and Kohn [1] established density functional theory (DFT) showing that the electron density, ρ , is all that is necessary to determine the exact energy of many electron systems. However, all the challenge of electronic structure is then moved into an unknown universal functional of the density, $\mathcal{F}[\rho]$. For a wavefunction, Ψ_v , that is the ground-state solution of the Schrödinger equation with potential v ,

$$E_v = \min_{\Psi} \langle \Psi | \hat{H} | \Psi \rangle = \langle \Psi_v | T + V_{ee} | \Psi_v \rangle + \text{Tr}(\rho_v v) \quad (1)$$

simply subtracting off the one-electron term, gives the exact Hohenberg-Kohn functional for ρ_v ($\Psi_v \rightarrow \rho_v$)

$$\mathcal{F}^{\text{HK}}[\rho_v] = E_v - \text{Tr}(\rho_v v) = \langle \Psi_v | T + V_{ee} | \Psi_v \rangle. \quad (2)$$

This procedure can be carried out for many different v , to obtain many points of the exact functional $\mathcal{F}^{\text{HK}}[\rho_v]$. A question arises of whether all possible densities are achievable. This is the problem of v -representability, that is addressed by the constrained search by Levy and Lieb [2, 3] following earlier work by Percus [4]

$$\mathcal{F}^{\text{Levy}}[\rho] = \min_{\Psi \rightarrow \rho} \langle \Psi | T + V_{ee} | \Psi \rangle. \quad (3)$$

This functional is defined for all possible densities coming from a N -electron wavefunction, including those that are not obtainable as the ground-state solution of a Schrödinger equation (not v -representable). Once the exact functional is known, the total energy is obtained by minimization only over densities,

$$E_v[\rho] = \min_{\rho} \{ \mathcal{F}[\rho] + \text{Tr}(\rho v) \}. \quad (4)$$

The exact functional of the first-order density matrix, γ , can be derived [2, 5]

$$F^{\text{Levy}}[\gamma] = \min_{\Psi \rightarrow \gamma} \langle \Psi | V_{ee} | \Psi \rangle, \quad (5)$$

and used similarly, where the kinetic energy term is now a known linear functional of γ

$$E_v[\rho] = \min_{\gamma} \{ F[\gamma] + \text{Tr}(\mathbf{T}\gamma) + \text{Tr}(v\gamma) \}. \quad (6)$$

In this Letter, the nature of the exact first-order density matrix functional is revealed by considering the asymmetric two-site Hubbard model. In this universe, the fundamental equations are tractable and the exact functional becomes a visualizable three dimensional energy landscape in the space of density matrices. We demonstrate how this one universal landscape gives the exact energy of all possible systems, for all numbers of electrons including fractional. This connected view of the functional for all density matrices makes clear the reasons for the failure of approximate functionals, and allows us to answer the questions of whether there are density-matrices which are not v -representable and also how the derivatives of the exact functional give the fundamental gap.

The asymmetric two-site Hubbard [6] model describes interacting electrons on a lattice of two sites that contains the physics of electron transfer and has even recently been experimentally described using two ultracold fermionic atoms [7]. It has the Hamiltonian

$$\hat{H} = -t \sum_{\sigma} \left(c_{1\sigma}^{\dagger} c_{2\sigma} + c_{2\sigma}^{\dagger} c_{1\sigma} \right) + U \sum_i \hat{n}_{i\alpha} \hat{n}_{i\beta} + \sum_{i\sigma} \epsilon_i \hat{n}_{i\sigma} \quad (7)$$

where the site index $i = 1, 2$, spin index $\sigma = \alpha, \beta$ and the number operator is $\hat{n}_{i\sigma} = c_{i\sigma}^{\dagger} c_{i\sigma}$. There has been recent work on the exact functional in this model from Fuks *et al* [8, 9], Carrascal *et al* [10], Pastor and coworkers [11, 12], Requist *et al* [13], and in other systems [14–16].

The parameters that define a particular model are the hopping between the sites, t , on-site energies ϵ_1/ϵ_2 and

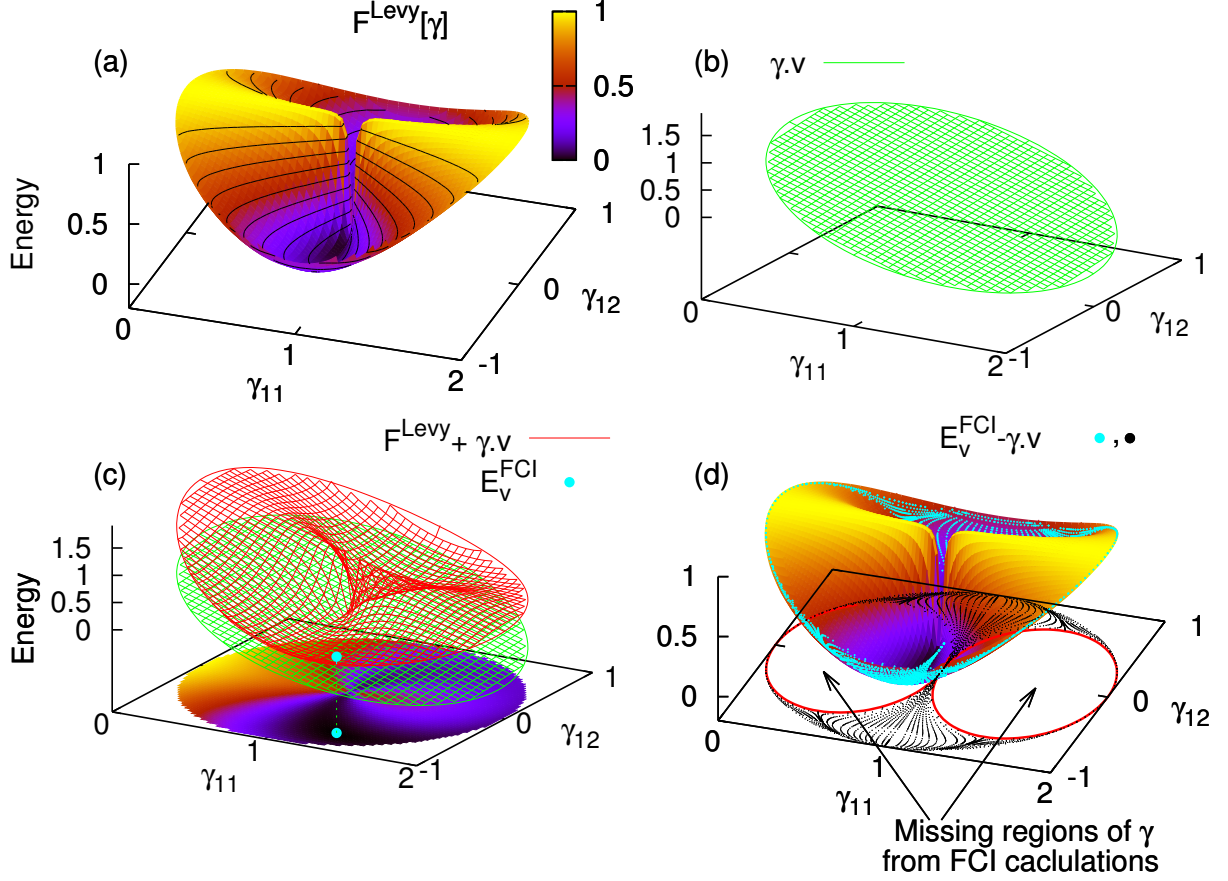


Figure 1: Energy landscape of the exact functional (a) $F^{\text{Levy}}[\gamma]$ for all allowable density matrices of the two site Hubbard model. (b) The one electron term, $\gamma.v$, for $t = 0.1$ and $\Delta\epsilon = 0.9$, which is purely a flat plane. (c) Illustration of the minimization of the exact functional adding on the same $\gamma.v$ term to give the FCI energy and density matrix, $\{E_v^{\text{FCI}}, \gamma_v^{\text{FCI}}\}$. (d) $F^{\text{Levy}}[\gamma]$ and 6552 points of $\{F^{\text{HK}}[\gamma_v^{\text{FCI}}], \gamma_v^{\text{FCI}}\}$ that show the E_v^{FCI} subtracting the one electron term (Eq. 11) at γ_v^{FCI} for many different v .

the electron-electron repulsion penalty due to double occupation of a site, U . The physics is completely determined by $\Delta\epsilon = \epsilon_1 - \epsilon_2$ and the ratio U/t , therefore, in this work U is fixed at 1 and t and $\Delta\epsilon$ are the chosen variables. The kinetic and on-site potential part of the Hamiltonian, which together we denote as v , is a real symmetric 2x2 matrix defined by parameters t and $\Delta\epsilon$

$$v = \begin{pmatrix} \Delta\epsilon/2 & -t \\ -t & -\Delta\epsilon/2 \end{pmatrix} \quad (8)$$

and the 2x2 density matrix, $\gamma_{ij} = \sum_{\sigma} \langle \Psi | c_{i\sigma}^{\dagger} c_{j\sigma} | \Psi \rangle$ is

$$\gamma = \begin{pmatrix} \gamma_{11} & \gamma_{12} \\ \gamma_{12}^* & (2 - \gamma_{11}) \end{pmatrix} \quad (9)$$

leading to a total energy for real density matrices

$$E_v = -2\gamma_{12}t + \gamma_{11}\Delta\epsilon/2 - (2 - \gamma_{11})\Delta\epsilon/2 + F[\gamma] \quad (10)$$

The exact functional can be obtained and understood from different perspectives. Firstly, for any γ that comes

from an exact diagonalization full configuration interaction (FCI) calculation with one-electron Hamiltonian v , the Hohenberg-Kohn functional is given by

$$F^{\text{HK}}[\gamma_v] = E_v^{\text{FCI}} + 2\gamma_{12}t - \gamma_{11}\Delta\epsilon/2 + (2 - \gamma_{11})\Delta\epsilon/2. \quad (11)$$

The second way is the constrained search over real singlet wavefunctions

$$\Psi = \frac{a}{\sqrt{2}} [\mathcal{A}(\phi_1\alpha\phi_2\beta) + \mathcal{A}(\phi_2\alpha\phi_1\beta)] + b\mathcal{A}(\phi_1\alpha\phi_1\beta) + c\mathcal{A}(\phi_2\alpha\phi_2\beta) \quad (12)$$

which can be simplified to an expression (see Refs. [10, 12] and supplementary information (SI) for more details)

$$F^{\text{Levy}}[\gamma] = \frac{\gamma_{12}^2 (1 - \sqrt{1 - \gamma_{12}^2 - [\gamma_{11} - 1]^2}) + 2[\gamma_{11} - 1]^2}{2(\gamma_{12}^2 + [\gamma_{11} - 1]^2)}. \quad (13)$$

Thirdly, it can be viewed as the exact functional in density matrix functional theory for two electrons. From the

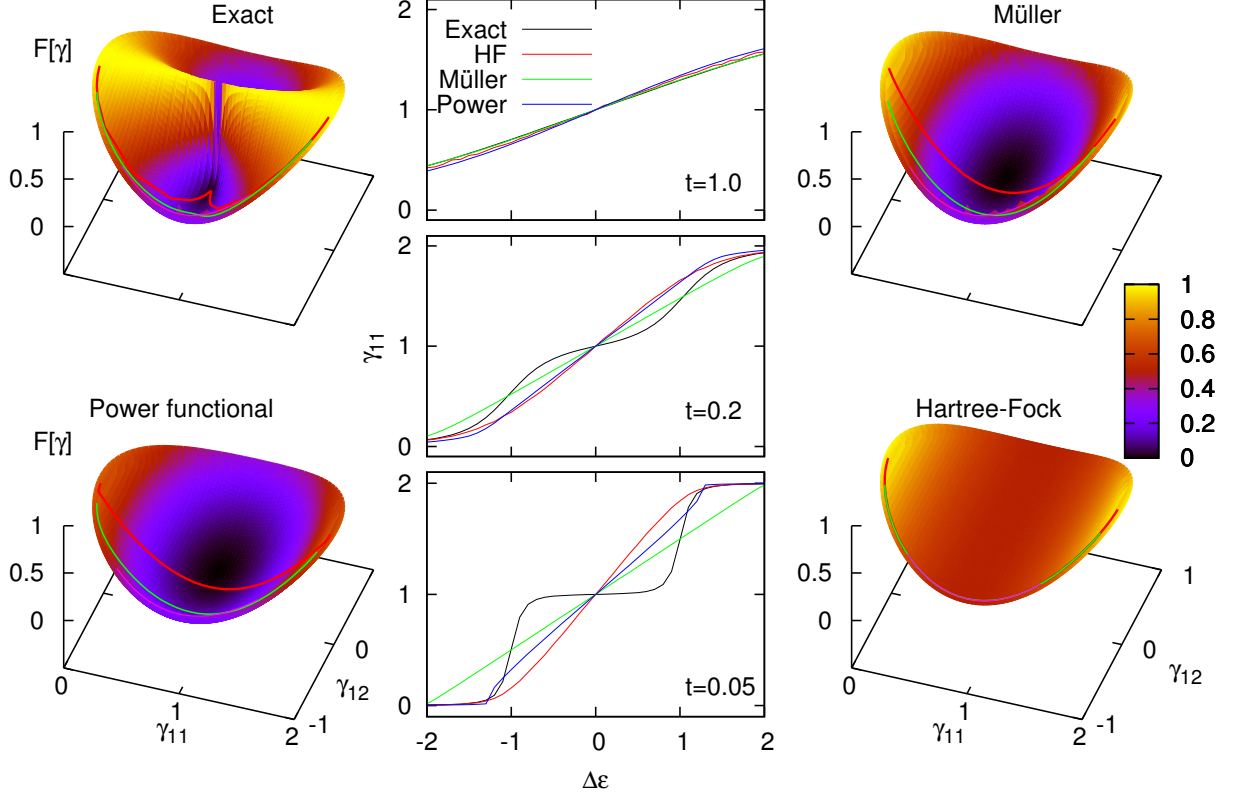


Figure 2: Entire landscape of $F[\gamma]$ for the exact functional, and three approximate density-matrix functionals (see supplementary information for more details). The minimizing values $\{F[\gamma_v], \gamma_v\}$ for three lines of v ($-2 \leq \Delta\epsilon < 2$) with $t = 1, 0.2, 0.05$ are plotted on the surfaces in purple, green and red, respectively. The central plots show the failure of approximate functionals to correctly describe the electron transfer (γ_{11} vs $\Delta\epsilon$) as t approaches the strongly correlated limit (see supplementary animations).

work of Löwdin and Shull in 1956 [17] using the natural orbitals $|a\rangle$ and $|b\rangle$ ($|p\rangle = \sum_{i=1,2} C_{pi} c_i^\dagger |\text{vac}\rangle$) and their occupation numbers n_a and n_b that diagonalize γ , it can be derived that

$$F^{\text{LS}}[\gamma] = \frac{1}{2} n_a \langle aa|aa \rangle + \frac{1}{2} n_b \langle bb|bb \rangle - \sqrt{n_a n_b} \langle aa|bb \rangle \quad (14)$$

where the two-electron integral is $\langle pp|qq \rangle = U \sum_{i=1,2} C_{pi}^2 C_{qi}^2$. This gives exact agreement with the constrained search expression, Eq. (13) and has been utilized in functionals such as the AGP natural orbital functional [18, 19] and PNOF5 [20] (see SI). There are two further possible routes to the exact functional (details in the SI): the extension over pure-state wavefunctions to complex, and the Lieb maximization[3], $F^{\text{Lieb}}[\gamma] = \sup_v \{E_v - \gamma.v\}$.

$F^{\text{Levy}}[\gamma]$ is shown in Fig. 1a. for the allowable density matrices $(\gamma_{11} - 1)^2 + \gamma_{12}^2 \leq 1$. It is represented as a unique surface of hills and a valley in a bowl type shape, with a channel through the centre (at $\gamma_{11} = 1$) and hills on both sides (reaching 1 at $\gamma_{12} = 0$). This defines the energy landscape that maps every possible system to its corresponding exact energy.

The exact functional is an energy landscape with only

one minimum, so how does it give rise to all possible FCI energies? This can be pictured in a very physical manner by considering a walk on this landscape, placed upon a flat surface tilted to the angle given by the one-electron potential, which gives a valley whose minimum equals exactly the FCI solution. Fig. 1b shows the one electron term for a particular v , defined by $t = 0.1$ and $\Delta\epsilon = 0.9$, and Fig. 1c shows the addition of this with the exact functional, $F^{\text{Levy}}[\gamma] + \gamma.v$, whose minimum is at the FCI energy, E_v^{FCI} , and FCI density matrix, γ_v . This holds for every possible v . Thus, once the exact functional is known, it gives the exact solution of any system by means of an almost trivial calculation.

We have performed a large number of FCI calculations varying the two free parameters, $-10 < t < 10$ and $-10 < \Delta\epsilon < 10$. Fig. 1d illustrates the result of over 6000 FCI calculations subtracting off the one electron term, $\gamma.v$, to give the $F^{\text{HK}}[\gamma]$ of Eq. (11). Every single light blue dot, representing many $F^{\text{HK}}[\gamma_v]$, lies on the surface of $F^{\text{Levy}}[\gamma]$. However, the one-particle density matrices γ_v that result from all these FCI calculations cover only a small fraction of the space (seen as the black dots projected onto the base of the plot with more

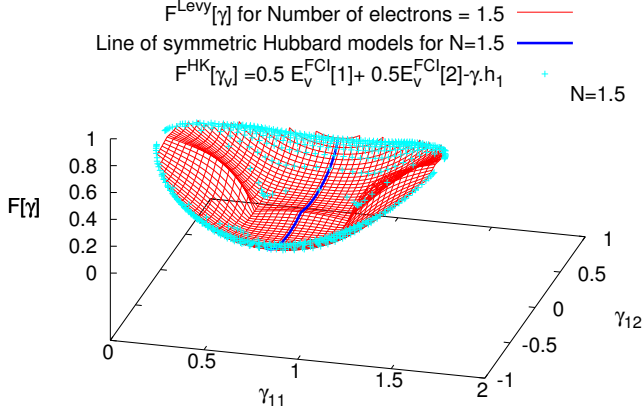


Figure 3: The exact functionals of Eqs (17) and (18) for $N = 1.5$ electrons, which gives back the exact energy of every system with 1.5 electrons.

details in SI). The rest of the density matrices are not v -representable, even though they are N -representable. From the perspective of the exact functional, it is clear why these density matrices can never be found, as they correspond to the hills of the surface where the $F^{\text{Levy}}[\gamma]$ lies inside a convex containing surface (see SI). Addition of the one electron interaction term, which is purely linear in the variables γ_{11} and γ_{12} , as pictured in Fig. 1b, means that these points can never be minima, and hence cannot be a FCI solution. In terms of the functional it corresponds to where the second derivatives of the functional are no longer positive definite as seen by the a negative lowest eigenvalue of the Hessian matrix of second derivatives, $H_{ij} = \frac{\partial^2 F}{\partial \gamma_{1i} \partial \gamma_{1j}}$, (see SI). It should also be noted that the lowest energy wavefunctions of the non- v -representable density matrices cannot be written in a Gutzwiller form [21] (see SI). The non- v -representable region highlights the key distinction between $F^{\text{Levy}}[\gamma]$ derived from pure-state wavefunctions, which can be concave, versus the $F^{\text{Lieb}}[\gamma]$ functional derived from ensembles by a Legendre-Fenchel transform, which is proven to be everywhere convex [3].

The derivatives of the functional (expressions in SI) satisfy the Euler equation and give the one-electron Hamiltonian needed,

$$\frac{\partial F[\gamma]}{\partial \gamma} = -v + C. \quad (15)$$

Now, consider the physics of electron transfer, by varying $\Delta\epsilon$, from the weakly correlated ($U/t = 1$) to strongly correlated ($U/t = 20$) regimes as depicted in Fig. 2. Correctly describing this electron transfer in the strongly correlated regimes is one of the great challenges of electronic structure, as demonstrated in Fig. 2 by the failure of approximate density matrix functionals such as Müller [22] and Power functionals [23]. The approximate functionals do not correctly describe the entire landscape and

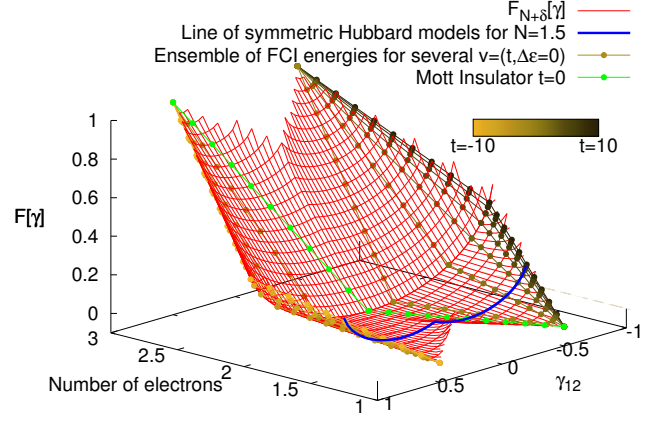


Figure 4: The exact functionals of Eqs. (17) and (18) for all numbers of electrons ($1 \leq N \leq 3$) in the symmetric two site Hubbard model.

thus completely fail to describe electron transfer (see animation in SI). This is related to the complete failure of all currently used density functionals for the electron transfer in a two-electron molecular type challenge (see HZ^{2e} of Ref. [24]).

The exact functional can be calculated for all numbers of electrons ($0 \leq N \leq 4$); the integer parts are trivial and given in the SI. For non-integer numbers of electrons, the functional is constructed using the Perdew, Parr, Levy and Balduz (PPLB)[25] ensemble extension to search over many-electron density matrices

$$\Gamma_{N+\delta} = c_0|\Psi_0\rangle\langle\Psi_0| + c_1|\Psi_1\rangle\langle\Psi_1| + c_2|\Psi_2\rangle\langle\Psi_2| + c_3|\Psi_3\rangle\langle\Psi_3| + c_4|\Psi_4\rangle\langle\Psi_4| \quad (16)$$

with $\sum_i c_i = 1$ and $\sum_i c_i \cdot i = N + \delta$ ($0 \leq \delta \leq 1$). Thus, we explicitly construct the fractional extension

$$F_{N+\delta}[\gamma] = \min_{\Gamma_{N+\delta} \rightarrow \gamma} \text{Tr}[\Gamma_{N+\delta} V_{ee}], \quad (17)$$

where, unlike PPLB, we have not assumed convexity of the energy versus N . That is, rather than using $\Gamma_{N+\delta} = c_N|\Psi_N\rangle\langle\Psi_N| + c_{N+1}|\Psi_{N+1}\rangle\langle\Psi_{N+1}|$, we explicitly search over ensembles of all N -electron wavefunctions ($N = 0, 1, 2, 3$, and 4) as in Eq. (16) (see SI).

Fig. 3 shows the extension of the exact functional to fractional numbers of electrons for $N + \delta = 1.5$. We obtained $F_{N+\delta}[\gamma]$ for all the possible density matrices, where the minimum is actually given only by the combination of N and $N + 1$ (see supplementary information for more details). We also find that all the appropriate ensembles of FCI energies subtracting off the one electron term using the ensemble of density matrices,

$$F_{N+\delta}^{\text{HK}}[v] = (1 - \delta)E_v^{\text{FCI}}[N] + \delta E_v^{\text{FCI}}[N + 1] - [(1 - \delta)\gamma_v^N + \delta\gamma_v^{N+1}] \cdot v \quad (18)$$

lie perfectly on the functional surface for all values of v and δ . Additionally, just like for integer electrons, a walk

on this surface tilted to the angle of any one-electron potential (analogously to Fig. 1c) gives a minimum point that exactly agrees with the ensemble FCI energy.

The knowledge of the exact functional for fractional numbers of electrons connects to the band-gap problem. This is the question of whether the fundamental gap, defined as the difference of the ionization energy and electron affinity, can be given by the derivatives of the exact functional. For simplicity, consider only the symmetric Hubbard dimer with different numbers of electrons. In Fig. 4 the exact functional is shown for $1 \leq N \leq 3$, along with several points of the ensemble $F_{N+\delta}^{\text{HK}}[v]$ with $v = \{-1 < t < 1, \Delta\epsilon = 0\}$ (see also animations in SI). For every v , $F_{N+\delta}^{\text{HK}}[v]$ traces out a straight line versus particle number with a clear derivative discontinuity at $N = 2$, hence the derivatives of the exact functional give the contribution to the fundamental gap

$$\left. \frac{\partial F[\gamma]}{\partial N_+} \right|_v - \left. \frac{\partial F[\gamma]}{\partial N_-} \right|_v = F[\gamma^{N+1}] + F[\gamma^{N-1}] - 2F[\gamma^N]. \quad (19)$$

If there is no discontinuity in the density matrix, which is the case of a Mott insulator, the entirety of the fundamental gap is given by the exact functional (Eq. 19). This is illustrated as the green line in Fig. 4 for the symmetric Hubbard model with $t = 0$ and $1 \leq N \leq 3$, and has a direct correspondence to the gap of infinitely stretched H_2 [26]. Nevertheless, most systems have a discontinuity in the density matrix, $\gamma^{N+1} - \gamma^N \neq \gamma^N - \gamma^{N-1}$, giving rise to a discontinuous derivative even for the one electron term, which is an entirely smooth flat plane. However, the direction in which γ changes upon electron addition or removal is already determined by derivatives of F whilst keeping the derivative in the direction of fixed N to be constant

$$\gamma_{N\pm 1} = \gamma_N + \frac{\delta\gamma}{\delta N_{\pm}} \bigg|_{\frac{\partial F}{\partial \gamma}|_N}. \quad (20)$$

Hence, the fundamental gap is solely determined by the derivatives of the functional itself,

$$\begin{aligned} \text{Gap}[\gamma_N] = & \left(\left. \frac{\partial F[\gamma]}{\partial N_+} \right|_{\frac{\partial F[\gamma]}{\partial \gamma}|_N} - \left. \frac{\partial \gamma}{\partial N_+} \right|_{\frac{\partial F}{\partial \gamma}|_N} \cdot \left. \frac{\partial F[\gamma]}{\partial \gamma} \right|_N \right) \\ & - \left(\left. \frac{\partial F[\gamma]}{\partial N_-} \right|_{\frac{\partial F[\gamma]}{\partial \gamma}|_N} - \left. \frac{\partial \gamma}{\partial N_-} \right|_{\frac{\partial F}{\partial \gamma}|_N} \cdot \left. \frac{\partial F[\gamma]}{\partial \gamma} \right|_N \right) \end{aligned}$$

Overall, it is amazing to have a universe that turns any question about the exact functional into simple movements of a three-dimensional energy landscape. Walks on this landscape and its valley and hills correspond to important physical concepts such as the exact energies of every possible system and domains of non- v -representable density matrices. Furthermore, in the direction of changing particle number there is a continuous surface that has

a derivative discontinuity at the integers, giving all possible fundamental gaps, including Mott insulators. The whole landscape of the exact functional is itself an infinite number of exact constraints, such that any approximation must approach and be mathematically proximal to it for the entire universe. It is this connected view of the exact functional for a family of densities in a global landscape that truly highlights a path for the improvement of approximate functionals.

We gratefully acknowledge funding from Ramon y Cajal (PMS) and the Royal Society (AJC). PMS also acknowledges grant FIS2012-37549 from the Spanish Ministry of Science.

-
- [1] P. Hohenberg and W. Kohn, Phys. Rev. **136**, B864 (1964).
 - [2] M. Levy, Proc. Natl. Acad. Sci. USA **76**, 6062 (1979).
 - [3] E. H. Lieb, Int. J. Quant. Chem. **24**, 243 (1983).
 - [4] J. K. Percus, Int. J. Quant. Chem. **13**, 89 (1978).
 - [5] T. L. Gilbert, Phys. Rev. B, 2111 (1975).
 - [6] J. Hubbard, Proc. R. Soc. A **276**, 238 (1963).
 - [7] S. Murmann, A. Bergschneider, V. M. Klinkhamer, G. Zürn, T. Lompe, and S. Jochim, Phys. Rev. Lett. **114**, 080402 (2015).
 - [8] J. I. Fuks, M. Farzanehpour, I. V. Tokatly, H. Appel, S. Kurth, and A. Rubio, Phys. Rev. A **88**, 062512 (2013).
 - [9] J. I. Fuks and N. T. Maitra, Phys. Chem. Chem. Phys. **16**, 14504 (2014).
 - [10] D. J. Carrascal, J. Ferrer, J. C. Smith, and K. Burke, J. Phys. Condens. Matter **27**, 393001 (2015).
 - [11] R. López-Sandoval and G. M. Pastor, Phys. Rev. B **66**, 155118 (2002).
 - [12] M. Saubanière and G. M. Pastor, Phys. Rev. B **84**, 035111 (2011).
 - [13] R. Requist and O. Pankratov, Phys. Rev. B **77**, 235121 (2008).
 - [14] A. M. Teale, S. Coriani, and T. Helgaker, J. Chem. Phys. **132**, 164115 (2010).
 - [15] S. Kvaal, U. Ekström, A. M. Teale, and T. Helgaker, J. Chem. Phys. **140**, 18A518 (2014).
 - [16] L. O. Wagner, T. E. Baker, E. M. Stoudenmire, K. Burke, and S. R. White, Phys. Rev. B **90**, 045109 (2014).
 - [17] P.-O. Löwdin and H. Shull, Phys. Rev. **101**, 1730 (1956).
 - [18] B. Barbiellini, J. Phys. Chem. Solids **61**, 341 (2000).
 - [19] B. Barbiellini and A. Bansil, J. Phys. Chem. Solids **62**, 2181 (2001).
 - [20] M. Piris, X. Lopez, F. Ruipérez, J. M. Matxain, and J. M. Ugalde, J. Chem. Phys. **134**, 164102 (2011).
 - [21] M. C. Gutzwiller, Phys. Rev. Lett. **10**, 159 (1963).
 - [22] A. Müller, Phys. Lett. A **105**, 446 (1984).
 - [23] S. Sharma, J. K. Dewhurst, N. N. Lathiotakis, and E. K. U. Gross, Phys. Rev. B **78**, 201103 (2008).
 - [24] P. Mori-Sánchez and A. J. Cohen, Phys. Chem. Chem. Phys. **16**, 14378 (2014).
 - [25] J. P. Perdew, R. G. Parr, M. Levy, and J. L. Balduz Jr., Phys. Rev. Lett. **49**, 1691 (1982).
 - [26] P. Mori-Sánchez, A. J. Cohen, and W. T. Yang, Phys. Rev. Lett. **102**, 066403 (2009).

Supplementary Information to "Landscape of an exact functional"

Aron J. Cohen

Department of Chemistry, Lensfield Rd, University of Cambridge, Cambridge, CB2 1EW, UK

Paula Mori-Sánchez

Departamento de Química and Instituto de Física de la Materia Condensada (IFIMAC), Universidad Autónoma de Madrid, 28049, Madrid, Spain

A. Derivation of Eq. (13)

To derive the exact functional,

$$F^{\text{Levy}} = \min_{\Psi \rightarrow \gamma} \langle \Psi | V_{ee} | \Psi \rangle \quad (\text{S1})$$

consider the minimization over real singlet wavefunctions

$$\begin{aligned} \Psi = & \frac{a}{\sqrt{2}} [\mathcal{A}(\phi_1 \alpha \phi_2 \beta) + \mathcal{A}(\phi_2 \alpha \phi_1 \beta)] \\ & + b \mathcal{A}(\phi_1 \alpha \phi_1 \beta) + c \mathcal{A}(\phi_2 \alpha \phi_2 \beta). \end{aligned} \quad (\text{S2})$$

in terms of the parameters a, b and c along with the normalization $a^2 + b^2 + c^2 = 1$ and the elements of the density-matrix $\gamma_{ij} = \sum_{\sigma} \langle \Psi | c_{i\sigma}^{\dagger} c_{j\sigma} | \Psi \rangle$ giving $\gamma_{11} = 2b^2 + a^2$ and $\gamma_{12} = \sqrt{2}(ba + ac)$. The two-electron energy comes only from the $\langle 11|11 \rangle$ and $\langle 22|22 \rangle$ integrals, which are U , as all other integrals are 0, so only the second determinant with itself and the third determinant with itself contribute, giving

$$F[\Psi] = U(b^2 + c^2) = U(1 - a^2) \quad (\text{S3})$$

It is also satisfied that

$$\gamma_{11} - 1 = b^2 - c^2. \quad (\text{S4})$$

Therefore, using γ_{12} gives

$$(b + c) = \frac{\gamma_{12}}{\sqrt{2}a} \quad (\text{S5})$$

and combining with Eq. (S4) leads to

$$(b - c) = \frac{(\gamma_{11} - 1) \sqrt{2}a}{\gamma_{12}} \quad (\text{S6})$$

Now, square Eqs. (S5) and (S6), to give

$$(b + c)^2 = \frac{\gamma_{12}^2}{2a^2} \quad (\text{S7})$$

and

$$(b - c)^2 = \frac{(\gamma_{11} - 1)^2 2a^2}{\gamma_{12}^2}. \quad (\text{S8})$$

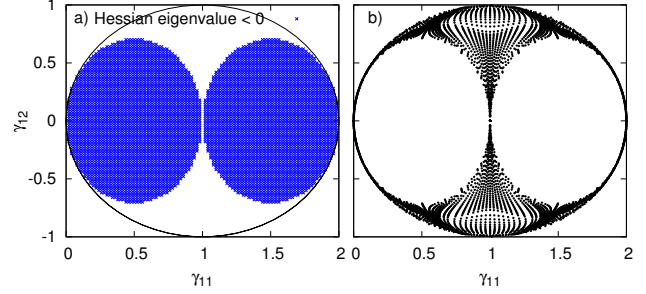


Figure S1: The plane of all possible density matrices illustrating the non- v -representability of many of the allowable γ . a) The second derivatives of the exact functional showing the points where the lowest hessian eigenvalue is < 0 from Eqs S14-S16 and b) the density matrices, γ , achieved in 6552 FCI calculations for $-10 < t < 10$ and $-10 < \Delta\epsilon < 10$.

Adding these two has the result

$$2b^2 + 2c^2 = \frac{\gamma_{12}^2}{2a^2} + \frac{(\gamma_{11} - 1)^2 2a^2}{\gamma_{12}^2}. \quad (\text{S9})$$

Using the normalization, gives

$$(2 - 2a^2) = \frac{\gamma_{12}^2}{2a^2} + \frac{(\gamma_{11} - 1)^2 2a^2}{\gamma_{12}^2} \quad (\text{S10})$$

which leads to a quadratic equation for a^2

$$\frac{[(\gamma_{11} - 1)^2 + \gamma_{12}^2]}{\gamma_{12}^2} a^4 - a^2 + \frac{\gamma_{12}^2}{4} = 0 \quad (\text{S11})$$

with solution

$$a^2 = \frac{\gamma_{12}^2 \left(1 \pm \sqrt{1 - (\gamma_{11} - 1)^2 - \gamma_{12}^2} \right)}{2[(\gamma_{11} - 1)^2 + \gamma_{12}^2]}. \quad (\text{S12})$$

Taking the plus combination gives the lowest energy

$$\begin{aligned} E &= 1 - a^2 \\ &= 1 - \frac{\gamma_{12}^2 \left(1 + \sqrt{1 - (\gamma_{11} - 1)^2 - \gamma_{12}^2} \right)}{2[(\gamma_{11} - 1)^2 + \gamma_{12}^2]} \\ &= \frac{2[(\gamma_{11} - 1)^2 + \gamma_{12}^2] - \gamma_{12}^2 \left(1 + \sqrt{1 - (\gamma_{11} - 1)^2 - \gamma_{12}^2} \right)}{2[(\gamma_{11} - 1)^2 + \gamma_{12}^2]} \end{aligned}$$

$$= \frac{2(\gamma_{11} - 1)^2 + \gamma_{12}^2 \left(1 - \sqrt{1 - (\gamma_{11} - 1)^2 - \gamma_{12}^2}\right)}{2[(\gamma_{11} - 1)^2 + \gamma_{12}^2]}. \quad (\text{S13})$$

The derivatives of the exact functional can be evaluated analytically and are used in Fig. S1.

This agrees with Eq. (13) of the paper.

$$\frac{\partial E}{\partial \gamma_{11}} = \frac{4(\gamma_{11} - 1) + (\gamma_{11} - 1)\gamma_{12}^2/\sqrt{1 - (\gamma_{11} - 1)^2 - \gamma_{12}^2}}{2((\gamma_{11} - 1)^2 - \gamma_{12}^2)} - \frac{(\gamma_{11} - 1) \left(2(\gamma_{11} - 1)^2 + \gamma_{12}^2 \left(1 - \sqrt{1 - (\gamma_{11} - 1)^2 - \gamma_{12}^2}\right)\right)}{[(\gamma_{11} - 1)^2 + \gamma_{12}^2]^2}$$

and

$$\begin{aligned} \frac{\partial E}{\partial \gamma_{12}} &= \frac{\gamma_{12}^3/\sqrt{1 - (\gamma_{11} - 1)^2 - \gamma_{12}^2} + 2\gamma_{12} \left(1 - \sqrt{1 - (\gamma_{11} - 1)^2 - \gamma_{12}^2}\right)}{2((\gamma_{11} - 1)^2 + \gamma_{12}^2)} - \frac{2\gamma_{12}(\gamma_{11} - 1)^2 + \gamma_{12}^3\sqrt{1 - (\gamma_{11} - 1)^2 - \gamma_{12}^2}}{[(\gamma_{11} - 1)^2 + \gamma_{12}^2]^2}. \\ \frac{\partial^2 E}{\partial \gamma_{11}^2} &= \frac{-4(\gamma_{11} - 1)^2 ((\gamma_{11} - 1)^2 + \gamma_{12}^2) \left(\frac{\gamma_{12}^2}{\sqrt{-\gamma_{11}^2 + 2\gamma_{11} - \gamma_{12}^2}} + 4\right) + 8(\gamma_{11} - 1)^2 \left(2(\gamma_{11} - 1)^2 - \gamma_{12}^2 \left(\sqrt{-\gamma_{11}^2 + 2\gamma_{11} - \gamma_{12}^2} - 1\right)\right)}{2((\gamma_{11} - 1)^2 + \gamma_{12}^2)^3} \\ &+ \frac{((\gamma_{11} - 1)^2 + \gamma_{12}^2)^2 \left(4 - \frac{\gamma_{12}^2(\gamma_{12}^2 - 1)}{(-\gamma_{11}^2 + 2\gamma_{11} - \gamma_{12}^2)^{3/2}}\right) - 2((\gamma_{11} - 1)^2 + \gamma_{12}^2) \left(2(\gamma_{11} - 1)^2 - \gamma_{12}^2 \left(\sqrt{-\gamma_{11}^2 + 2\gamma_{11} - \gamma_{12}^2} - 1\right)\right)}{2((\gamma_{11} - 1)^2 + \gamma_{12}^2)^3} \quad (\text{S14}) \\ \frac{\partial^2 E}{\partial \gamma_{11} \partial \gamma_{12}} &= -\frac{(\gamma_{11} - 1)\gamma_{12} \left(-2\gamma_{11}^6 + 12\gamma_{11}^5 + 2\gamma_{11}^2 \left(10\sqrt{-\gamma_{11}^2 + 2\gamma_{11} - \gamma_{12}^2} - 9\gamma_{12}^2 + 1\right) - 4\gamma_{11} \left(2\sqrt{-\gamma_{11}^2 + 2\gamma_{11} - \gamma_{12}^2} - 3\gamma_{12}^2 + 1\right)\right)}{2(-\gamma_{11}^2 + 2\gamma_{11} - \gamma_{12}^2)^{3/2} (\gamma_{11}^2 - 2\gamma_{11} + \gamma_{12}^2 + 1)^3} \\ &- \frac{(\gamma_{11} - 1)\gamma_{12} \left(\gamma_{12}^2 \left(-2\gamma_{12}^2 \left(2\sqrt{-\gamma_{11}^2 + 2\gamma_{11} - \gamma_{12}^2} + 3\right) + 4\sqrt{-\gamma_{11}^2 + 2\gamma_{11} - \gamma_{12}^2} + \gamma_{12}^4 + 1\right)\right)}{2(-\gamma_{11}^2 + 2\gamma_{11} - \gamma_{12}^2)^{3/2} (\gamma_{11}^2 - 2\gamma_{11} + \gamma_{12}^2 + 1)^3} \\ &- \frac{(\gamma_{11} - 1)\gamma_{12} \left(+\gamma_{11}^4 \left(4 \left(\sqrt{-\gamma_{11}^2 + 2\gamma_{11} - \gamma_{12}^2} - 6\right) - 3\gamma_{12}^2\right) - 4\gamma_{11}^3 \left(4\sqrt{-\gamma_{11}^2 + 2\gamma_{11} - \gamma_{12}^2} - 3\gamma_{12}^2 - 4\right)\right)}{2(-\gamma_{11}^2 + 2\gamma_{11} - \gamma_{12}^2)^{3/2} (\gamma_{11}^2 - 2\gamma_{11} + \gamma_{12}^2 + 1)^3} \quad (\text{S15}) \\ \frac{\partial^2 E}{\partial^2 \gamma_{12}^2} &= \frac{-4\gamma_{12}^2 ((\gamma_{11} - 1)^2 + \gamma_{12}^2) \left(\frac{\gamma_{12}^2}{\sqrt{-\gamma_{11}^2 + 2\gamma_{11} - \gamma_{12}^2}} - 2\sqrt{-\gamma_{11}^2 + 2\gamma_{11} - \gamma_{12}^2} + 2\right)}{2((\gamma_{11} - 1)^2 + \gamma_{12}^2)^3} \\ &+ \frac{8\gamma_{12}^2 \left(2(\gamma_{11} - 1)^2 - \gamma_{12}^2 \left(\sqrt{-\gamma_{11}^2 + 2\gamma_{11} - \gamma_{12}^2} - 1\right)\right) - 2((\gamma_{11} - 1)^2 + \gamma_{12}^2) \left(2(\gamma_{11} - 1)^2 - \gamma_{12}^2 \left(\sqrt{-\gamma_{11}^2 + 2\gamma_{11} - \gamma_{12}^2} - 1\right)\right)}{2((\gamma_{11} - 1)^2 + \gamma_{12}^2)^3} \\ &+ \frac{((\gamma_{11} - 1)^2 + \gamma_{12}^2)^2 \left(\frac{5\gamma_{12}^2}{\sqrt{-\gamma_{11}^2 + 2\gamma_{11} - \gamma_{12}^2}} - 2\sqrt{-\gamma_{11}^2 + 2\gamma_{11} - \gamma_{12}^2} + \frac{\gamma_{12}^4}{(-\gamma_{11}^2 + 2\gamma_{11} - \gamma_{12}^2)^{3/2}} + 2\right)}{2((\gamma_{11} - 1)^2 + \gamma_{12}^2)^3} \quad (\text{S16}) \end{aligned}$$

For the discussion of v -representability, there are two common counterexamples: the first is a one-electron density with a certain type of cusp, given by Englisch and Englisch[1]; the other is a spherical p density related to a degeneracy that cannot be given by a single wavefunction[2]. The non- v -representable density matrices shown here are very different to these two examples

and are only due to the nature of the energy surface of the exact functional as shown in Fig. S2.

B. Derivation of Löwdin-Shull for Hubbard model

Löwdin and Shull (LS) showed that the natural orbitals, ϕ_k , that diagonalize the density matrix and wave-

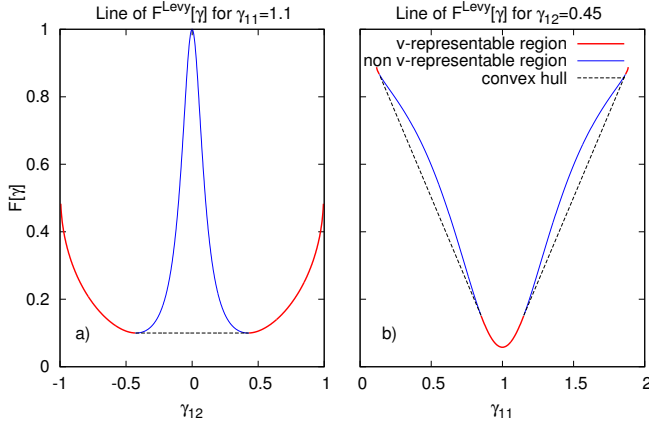


Figure S2: Two lines of $F^{\text{Levy}}[\gamma]$ that illustrate non- v -representable density matrices, due to the non convexity of the surface along the given line.

function for two electrons are the same

$$\Psi(\mathbf{r}, \mathbf{r}') = \sum_k c_k \phi_k(\mathbf{r}) \phi_k(\mathbf{r}') \quad (\text{S17})$$

$$\gamma(\mathbf{r}, \mathbf{r}') = \sum_k n_k \phi_k(\mathbf{r}) \phi_k(\mathbf{r}') \quad (\text{S18})$$

where $n_k = 2c_k^2$.

$$E^{\text{LS}}[\Psi] = \sum_{i=1}^2 c_i^2 \{2h_{ii} + \langle ii|ii \rangle\} + 2c_1 c_2 \langle 11|22 \rangle \quad (\text{S19})$$

For two basis functions the minimum energy wavefunction comes from the coefficients of c_1 and c_2 having opposite signs, $c_1 = \sqrt{n_1/2}$ and $c_2 = -\sqrt{n_2/2}$. Substituting this into the energy expression for the wavefunction gives an expression in terms of the natural orbitals and the natural orbital occupation numbers, n_k ,

$$F^{\text{LS}}[\gamma] = \frac{1}{2} n_a \langle aa|aa \rangle + \frac{1}{2} n_b \langle bb|bb \rangle - \sqrt{n_a n_b} \langle aa|bb \rangle. \quad (\text{S20})$$

There has been some recent interest in natural orbitals [3] and natural orbital functionals that, for two electron systems, must reduce to the Löwdin-Shull expression if they are to be exact, for example the PNOF5 functional [4–6].

The eigenvalues of the density matrix $\gamma = \begin{pmatrix} \gamma_{11} & \gamma_{12} \\ \gamma_{12} & (2 - \gamma_{11}) \end{pmatrix}$ are

$$(\gamma_{11} - n)((2 - \gamma_{11} - n) - \gamma_{12}^2) = 0 \quad (\text{S21})$$

$$n^2 - 2n + 2\gamma_{11} - \gamma_{11}^2 - \gamma_{12}^2 = 0 \quad (\text{S22})$$

$$n_{\pm} = \left(-2 \pm \sqrt{4 - 4(\gamma_{11} - 1)^2 + 4\gamma_{12}^2} \right) / 2 \quad (\text{S23})$$

$$n_{\pm} = n_{a/b} = 1 \pm \sqrt{(\gamma_{11} - 1)^2 + \gamma_{12}^2}. \quad (\text{S24})$$

The $\langle pp|qq \rangle$ integrals are in the natural orbital basis and the coefficients of the natural orbitals (C_{pi}) are found by substituting in the natural orbital numbers e.g. $(\gamma_{11} - n_p) C_{p1} + \gamma_{12} C_{p2} = 0$ or (also using $C_{\pm i} = C_{(a/b)i}$)

$$C_{\pm 1} = \frac{(\gamma_{11} - 1) \pm \sqrt{(\gamma_{11} - 1)^2 + \gamma_{12}^2}}{\gamma_{12}} C_{\pm 2} \text{ and } C_{\pm 1}^2 + C_{\pm 2}^2 = 1 \quad (\text{S25})$$

So overall, $C_{\pm 1}^2 = a_{\pm}^2 / (\gamma_{12}^2 + a_{\pm}^2)$ and $C_{\pm 2}^2 = \gamma_{12}^2 / (a_{\pm}^2 + \gamma_{12}^2)$ and hence

$$F^{\text{LS}} = \frac{1}{2} n_a (C_{a1}^4 + C_{a2}^4) U + \frac{1}{2} n_b (C_{b1}^4 + C_{b2}^4) U - \sqrt{n_a n_b} (C_{a1}^2 C_{b1}^2 + C_{a2}^2 C_{b2}^2) U. \quad (\text{S26})$$

For convenience, replace $r = (\gamma_{11} - 1)$ and $S = \sqrt{r^2 + \gamma_{12}^2}$, to obtain the following expression

$$F^{\text{LS}} = \frac{(1+S)}{2} \left[\left(\frac{(r+S)^2}{\gamma_{12}^2 + (r+S)^2} \right)^2 + \left(\frac{\gamma_{12}^2}{\gamma_{12}^2 + (r+S)^2} \right)^2 \right] + \frac{(1-S)}{2} \left[\left(\frac{(r-S)^2}{\gamma_{12}^2 + (r-S)^2} \right)^2 + \left(\frac{\gamma_{12}^2}{\gamma_{12}^2 + (r-S)^2} \right)^2 \right] - \sqrt{1-S^2} \left[\frac{(r+S)^2}{\gamma_{12}^2 + (r+S)^2} \frac{(r-S)^2}{\gamma_{12}^2 + (r-S)^2} + \frac{\gamma_{12}^2}{\gamma_{12}^2 + (r+S)^2} \frac{\gamma_{12}^2}{\gamma_{12}^2 + (r-S)^2} \right] \quad (\text{S27})$$

This equation could be simplified further but we have checked, by numerical evaluation with Fortran code, that it gives identical results to Eq. (13).

C. Complex

The constrained search $\Psi \rightarrow \gamma$ can be expanded over complex wavefunctions where the parameters, a, b, c , in

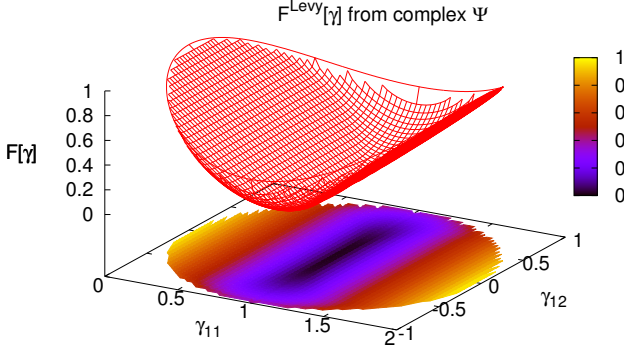


Figure S3: The exact functional allowing the wavefunction to be complex in the Levy search.

the wavefunction

$$\Psi = \frac{a}{\sqrt{2}} [\mathcal{A}(\phi_1\alpha\phi_2\beta) + \mathcal{A}(\phi_2\alpha\phi_1\beta)] + b\mathcal{A}(\phi_1\alpha\phi_1\beta) + c\mathcal{A}(\phi_2\alpha\phi_2\beta) \quad (\text{S28})$$

are allowed to be complex

$$\begin{aligned} a &= a_r + ia_i \\ b &= b_r + ib_i \\ c &= c_r + ic_i \end{aligned}$$

In terms of these parameters there are the following constraints:

$$\begin{aligned} 1 &= a_r^2 + a_i^2 + b_r^2 + b_i^2 + c_r^2 + c_i^2 \\ \gamma_{11} &= 2a_r^2 + 2a_i^2 + b_r^2 + b_i^2 \\ \Re(\gamma_{12}) &= \sqrt{2}(a_rb_r + a_ib_i + b_rc_r + b_ic_i) \end{aligned}$$

The imaginary part $\Im(\gamma_{12})$ can be anything as it does not enter the energy expression. A fourth constraint can be included if the overall phase of the wavefunction is set to zero.

We now carry out a search over all possible wavefunctions minimizing E and a given γ_{11} and $\Re(\gamma_{12})$, which gives Fig. S3. We do this by an explicit grid search over the two remaining variables for each γ_{11}, γ_{12} that is specified. The resulting energy functional gives the same result as the Hubbard expression Eq. (13) for all density matrices except the non- v -representable set. For all possible FCI density matrices it is, of course, in agreement with $F^{\text{HK}}[\gamma_v]$. For the non- v -representable set, $F_{\text{complex}}^{\text{Levy}}[\gamma]$ can be lower in energy, though this does not change any physics as these points can never be minima of any Hamiltonian. In this case, the functional numerically agrees with the ensemble functional considered by Saub  nere and Pastor[7] given by a density matrix that is an ensemble of two wavefunctions $\Gamma = a|\Psi_a\rangle\langle\Psi_a| + b|\Psi_b\rangle\langle\Psi_b|$. It should be noted that when

$F_{\text{complex}}^{\text{Levy}}[\gamma]$ is lower than Eq. (13) the solutions have a current and this may give a connection to the exact functional in current DFT (CDFT) [8, 9].

D. Lieb maximization

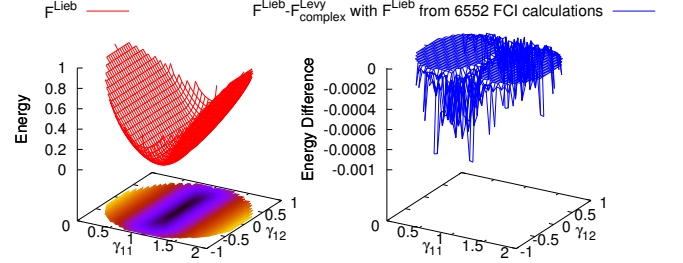


Figure S4: Functional $F^{\text{Lieb}}[\rho]$ from Lieb maximization using 6552 FCI calculations

Another way to calculate a bound for the functional is to perform the Lieb maximization[10],

$$F^{\text{Lieb}}[\gamma] = \sup_v \{E_v - \gamma \cdot v\} \quad (\text{S29})$$

which is a supremum (a smallest upper bound which for any finite set would just be a maximum) on the set of v . This means for a finite set it would actually be a lower bound to the true minimum $F^{\text{Lieb}}[\gamma] \leq F^{\text{Levy}}[\gamma]$. The Lieb maximization is carried out using 6552 FCI calculations for v , with $-10 < t < 10$ and $-10 < \Delta\epsilon < 10$. Over a grid of density matrices, we compare directly with $F_{\text{complex}}^{\text{Levy}}$ from complex wavefunctions as in the region of non- v -representable densities it is closest to the complex or ensemble form. Carrying out the maximization of Eq. (S29) gives the results in the left hand side of Fig. S4 and the difference to $F_{\text{complex}}^{\text{Levy}}$ is shown in the right-hand side. This difference is small and negative which illustrates that the Lieb maximization only gives a lower bound to the true functional that in this case is known exactly. Obviously, with more and more FCI calculations $F^{\text{Lieb}}[\gamma]$ would approach closer to the correct result. The $F^{\text{Lieb}}[\gamma]$ should not be used in minimizations in the same way as $F^{\text{Levy}}[\gamma]$ as it is a lower bound rather than an upper bound. Finally it should be noted that $F^{\text{Lieb}}[\gamma]$ is everywhere convex by construction and cannot, for example, contribute to the discussion on v -representability.

E. Approximate Density Matrix Functionals

We consider various approximate density matrix functionals including Hartree-Fock as a density matrix functional, Muller[11], Power [12]. Here the value of the natural orbital occupation numbers $0 \leq$

$n_i \leq 2$ and the two-electron integrals $\langle pq|rs \rangle = \int \int \phi_p^*(\mathbf{r})\phi_r(\mathbf{r})V_{ee}(\mathbf{r},\mathbf{r}')\phi_q^*(\mathbf{r}')\phi_s(\mathbf{r}')d\mathbf{r}d\mathbf{r}'$ which in the asymmetric two-site Hubbard model just work out to be $\langle pq|rs \rangle = \sum_{i=1,2} C_{pi}C_{qi}C_{ri}C_{si}$ in terms of the orbitals coefficients C_{pi} ($|p \rangle = \sum_{i=1,2} C_{pi}c_i^\dagger|\text{vac}\rangle$)

$$F^{\text{Hartree-Fock}} = \frac{1}{2}n_in_j\langle ij|ij \rangle - \frac{1}{4}n_in_j\langle ii|jj \rangle$$

$$F^{\text{Müller}} = \frac{1}{2}n_in_j\langle ij|ij \rangle - \frac{1}{2}\sqrt{n_in_j}\langle ii|jj \rangle$$

$$F^{\text{Power}} = \frac{1}{2}n_in_j\langle ij|ij \rangle - \frac{1}{2}(n_in_j)^\alpha\langle ii|jj \rangle$$

In the paper we use a value $\alpha = 0.675$ that has recently been used for Mott insulators

F. Gutzwiller approximate wavefunction

The Gutzwiller wavefunction [13] is a parametrized wavefunction of the form

$$\begin{aligned} \Psi &= \frac{1}{\sqrt{2}} [\mathcal{A}(\phi_1\alpha\phi_2\beta) + \mathcal{A}(\phi_2\alpha\phi_1\beta)] \\ &+ g[\mathcal{A}(\phi_1\alpha\phi_1\beta) + \mathcal{A}(\phi_2\alpha\phi_2\beta)] \end{aligned}$$

When $g = 1$ it is the Hartree-Fock wavefunction for orbitals $\phi = \frac{1}{\sqrt{2}}(\phi_1 + \phi_2)$. The basic idea is that in an H_2 like system as $g \rightarrow 0$ it goes to the Heitler-London wavefunction. In the asymmetric two-site Hubbard model we consider an orbital of the form $\phi = c_1\phi_1 + \sqrt{1 - c_1^2}\phi_2$ and a Gutzwiller wavefunction

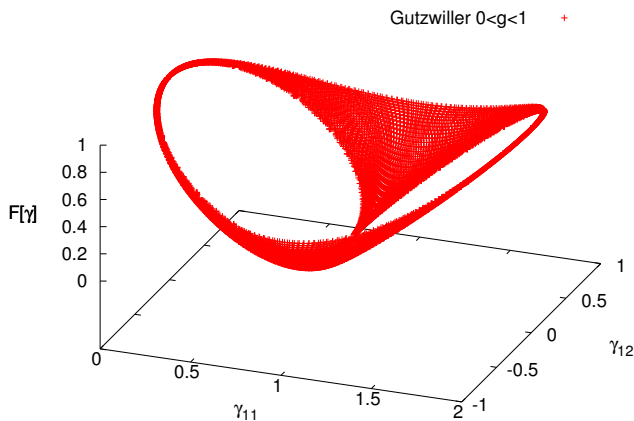


Figure S5:

$$\begin{aligned} \Psi^{\text{GWA}} &= \frac{2c_1\sqrt{1-c_1^2}}{\sqrt{2}} [\mathcal{A}(\phi_1\alpha\phi_2\beta) + \mathcal{A}(\phi_2\alpha\phi_1\beta)] \\ &+ g[c_1^2\mathcal{A}(\phi_1\alpha\phi_1\beta) + (1-c_1^2)\mathcal{A}(\phi_2\alpha\phi_2\beta)] \end{aligned}$$

If we consider all possible values of c_1 and $-1 \leq g \leq 1$ we get the following density matrices and

$$F[\Psi^{\text{GWA}}] = \frac{\langle \Psi^{\text{GWA}} | V_{ee} | \Psi^{\text{GWA}} \rangle}{\langle \Psi^{\text{GWA}} | \Psi^{\text{GWA}} \rangle}.$$

For other values of $|g| > 1$ the wavefunction is no longer a ground state wavefunction.

G. Functional for $N = 0, 1, 2, 3$ and 4

The functional is calculated for different integer numbers of electrons ($N = 0, 1, 2, 3$ and 4), where the trace of the density matrix $\gamma_{11} + \gamma_{22} = N$. At $N = 0$, $F[\gamma] = 0$ and there is only one allowed density matrix $\gamma_{11} = \gamma_{12} = 0$. For $N = 1$, $F[\gamma] = 0$ as there is no electron-electron interaction, however, the allowable density matrices from a pure state wavefunction are now defined by a circle $\gamma_{12} = \sqrt{(\gamma_{11} - 0.5)^2 - 0.5^2}$. Inside this circle are ensemble- N -representable density matrices but they cannot come from a pure-state wavefunction. For $N = 2$, $F[\gamma]$ is that of Eq. (13). For $N = 3$, $F[\gamma] = 1$ at the allowed pure-state density matrices defined by a different circle $\gamma_{12} = \sqrt{(\gamma_{11} - 1.5)^2 - 0.5^2}$. Also at $N = 4$, $F[\gamma] = 2$ at density matrix $\gamma_{11} = 2$, $\gamma_{12} = 0$. All these integer parts of the exact functional are pictured in the supplementary information.S6

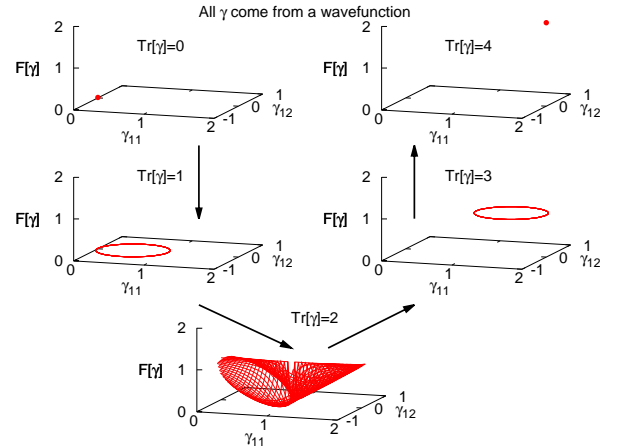


Figure S6: $F[\gamma]$ for $N = 0, 1, 2, 3, 4$ electrons

H. Other ensembles for $N = 1.5$ electrons

In the consideration of fractional numbers of electrons the argument of convexity of E vs N is often used to simplify the ensembles that have to be taken. If convexity

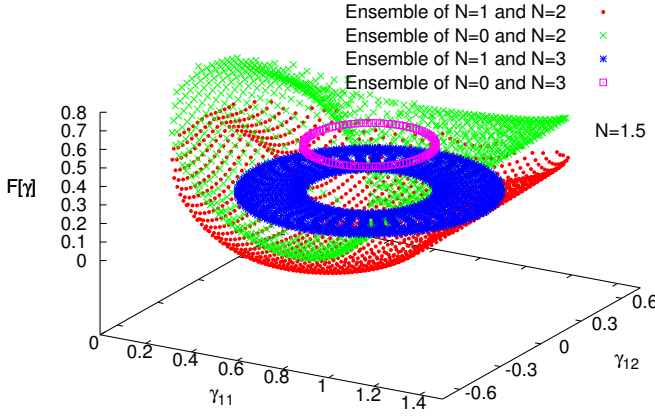


Figure S7: Different ensemble formation of $F[\gamma^{N=1.5}]$ combining pure state wavefunction for $N = 0, 1, 2, 3$ electrons

is true, the lowest energy ensemble will always be given by the combination of the two integers at either side, e.g. $\Gamma_{N+\delta} = (1 - \delta)\Gamma_N + \delta\Gamma_{N+1}$. However, convexity has not been proven, with definitely known counterexamples for certain electron-electron interactions, which indicates that most certainly convexity is not a general property of Hamiltonians [10]. Here, we test convexity for the two-site Hubbard hamiltonians, by taking ensembles of different electron numbers. We consider different pair-wise ensembles $\Gamma_{N=1.5} = a|\Psi_{n_1}\rangle\langle\Psi_{n_1}| + b|\Psi_{n_2}\rangle\langle\Psi_{n_2}|$ with $\{n_1, n_2\} = \{1, 2\}, \{0, 2\}, \{1, 3\}, \{0, 3\}$. We have also considered all possible ensembles, including those of three and four different particle numbers up to $N = 4$, all of these lie higher in energy.

[1] H. Englisch and R. Englisch, Physica A **121**, 253 (1983).

- [2] A. Savin, *Recent Developments and Applications of Modern Density Functional Theory* (ed J. M. Seminario, Elsevier, Amsterdam, 1996), p. 327.
- [3] K. J. H. Giesbertz and R. van Leeuwen, J. Chem. Phys. **139**, 104110 (2013).
- [4] M. Piris, X. Lopez, F. Ruipérez, J. M. Matxain, and J. M. Ugalde, J. Chem. Phys. **134**, 164102 (2011).
- [5] K. Pernal, Computational and Theoretical Chemistry **1003**, 127 (2013).
- [6] M. Piris, J. M. Matxain, and X. Lopez, J. Chem. Phys. **139**, 234109 (2013).
- [7] M. Saubanère and G. M. Pastor, Phys. Rev. B **84**, 035111 (2011).
- [8] G. Vignale and M. Rasolt, Phys. Rev. Lett. **59**, 2360 (1987).
- [9] E. I. Tellgren, S. Kvaal, E. Sagvolden, U. Ekström, A. M. Teale, and T. Helgaker, Phys. Rev. A **86**, 062506 (2012).
- [10] E. H. Lieb, Int. J. Quant. Chem. **24**, 243 (1983).
- [11] A. Müller, Phys. Lett. A **105**, 446 (1984), ISSN 0375-9601.
- [12] S. Sharma, J. K. Dewhurst, N. N. Lathiotakis, and E. K. U. Gross, Phys. Rev. B **78**, 201103 (2008).
- [13] M. C. Gutzwiller, Phys. Rev. Lett. **10**, 159 (1963).

I. Supplementary Animations

Supplementary animated gifs can be found in the arXiv source file or currently available via the following hyperlinks

- 1) [Varying \$t\$ with fixed \$\Delta\epsilon\$](#)
- 2) [Electron transfer by varying \$\Delta\epsilon\$ for \$t = 1.0, 0.2, 0.05\$](#)
- 3) [Varying \$t\$ for fractional number of electrons, \$N\$](#)